1

What makes the control of discontinuous dynamical systems so complex?

Eva M. Navarro-López

School of Computer Science, The University of Manchester, Oxford Road, Kilburn Building, Manchester, M13 9PL, United Kingdom (`eva.navarro@cs.man.ac.uk`)

Summary. The control of complex engineering systems requires combining multi-disciplinary methods. The spirit of this work is to bring together dynamical-systems analysis tools and control-engineering methods. The aim is to identify safe operating conditions and propose control methodologies to suppress non-desired phenomena in an industrial application with discontinuous elements: a conventional vertical oilwell drillstring. Due to the discontinuous bit-rock friction in the drillstring, complex phenomena are present, giving rise to different types of harmful oscillations. Torsional mechanical vibrations are studied, in particular, self-excited stick-slip oscillations at the bottom-hole assembly and other bit sticking phenomena which make the bit remain motionless. The complexity of drilling mechanisms and practices makes difficult the use of automated-type controllers. Consequently, the control system must be interpreted as an off-line safe-parameter selection method which can guide the driller in order to design the well drilling profile. From the dynamical viewpoint, the drillstring is a discontinuous or switched dynamical system and exhibits different discontinuous-induced bifurcations. The analysis of dynamical transitions and discontinuity-induced bifurcations is carried out in order to ensure good performance of the controlled system. The sticking bit phenomena are related to the existence of a sliding motion on the discontinuity surface when the bit velocity is zero. Some control solutions and parameters selection methods are presented in order to avoid non-desired transitions. Although the model used is a simplified one of two degrees of freedom, the analysis carried out can be successfully applied to multi-degree-of-freedom mechanical systems exhibiting stick-slip oscillations and dry friction.

Key words: Discontinuous systems, dry friction, sliding motions, stick-slip, switched control systems, oilwell drillstrings, mechanical vibrations

1 Introduction

Is it possible to know with certainty the evolution of engineering systems? What makes the control of systems exhibiting some changing dynamics so complex? Does unexpected complexity arise from simplicity? Where does the unpredictible behaviour of complex systems come from: from the system itself, or from the environment?

The main source of problems in an electromechanical system is the onset of vibrations and friction-induced phenomena. From a dynamical viewpoint, these phenomena are the consequence of some switching behaviour or discontinuous changes in the system properties. The systems with this feature are called discontinuous, switched or non-smooth dynamical systems. In these systems, the trajectories evolve smoothly through the state space until some conditions are satisfied and an event is triggered inducing a change in the model characteristics. Due to the presence of discontinuous changes in system properties, discontinuous dynamical systems present a wide variety of complex dynamical behaviours. In this paper, an electromechanical discontinuous system is studied: a conventional vertical oilwell drillstring.

Oilwell drillstrings are an example of complex engineering systems. The interaction of the drillstring with the borehole gives rise to non-desired oscillations or vibrations due to the presence of different types of friction. Vibrations are inevitable in drilling operations. The grade of severity of them depends mainly on the design of the bottom-hole assembly (BHA), the borehole characteristics, and three key drilling parameters: the weight on the bit (WOB), the rotary velocity of the mechanism and the torque applied at the top-rotary system. The application of techniques of dynamical analysis and control in a drilling mechanism can help in the proposal of operation recommendations for the driller, as well as recommendations for the drillstring and the BHA designs in order to reduce the effects of the vibrations.

There are three types of drillstring mechanical vibrations, and different phenomena are associated to each type of vibration, mainly: torsional (phenomenon of stick-slip), axial (bit bouncing phenomenon), and lateral (whirl motion due to the out-of-balance of the drillstring). These phenomena are a source of components failures, which reduce penetration rates and increase drilling operation costs [1, 2, 3, 4]. Stick-slip friction-induced oscillations at the BHA and the permanent stuck-bit situation are particularly harmful [1, 5, 6, 7, 8]. One of the consequences of the bit stick-slip phenomenon is that the top-rotary system in the drillstring rotates with a constant speed, whereas the bit rotary speed varies between zero and up to six times the rotary speed measured at the surface.

Different control approaches have been so far proposed to reduce the effects of stick-slip oscillations in oilwell drillstrings. For example, [9, 10, 11] propose a vibration absorber at the top of the drillstring. In addition, a classical PID control structure at the surface is used in [4, 17, 12, 13]. More sophisticated techniques are used in [14] and [15] where a linear quadratic regulator and a linear H^∞ control are used, respectively. Recently in [20], an analysis of bifurcations and transitions between several bit dynamics has been reported for a drillstring with n-degree-of-freedoms (DOF). Changes in drillstring dynamics are analysed through variations in key drilling parameters. For more examples of modelling and control of drillstring oscillations, the reader is invited to see the references in [4, 16, 18, 20, 21, 22, 23].

This paper sums up some of the author's results concerning the dynamical analysis and control of bit sticking phenomena in conventional vertical oilwell drillstrings [4, 16, 17, 18, 19, 20, 21, 22, 23], and throws light on an alternative characterization of stick-slip oscillations in discontinuous mechanical systems with multiple degrees of freedom whose dynamical behaviour depends on the variation of multiple parameters.

The study is focused on the mechanism torsional behaviour and the effects of the bit-rock friction, that is, stick-slip oscillations at the BHA and other bit sticking phenomena which cause the bit to remain motionless. A lumped-parameter piecewise-smooth (PWS) model of 2-DOF is considered, which is a particular case of the generic n-DOF model proposed in [20]. All the results are valid for the general model of n-DOF, although the paper is restricted to the 2-DOF model for the sake of simplicity in the presentation of results. The bit-rock contact is modelled by means of a dry friction combined with an exponential decaying law, which introduces a discontinuity in the open-loop system. The author has also proposed a novel hybrid-type modelling framework to specify the dynamics of the class of systems presented from a computational viewpoint [24, 25].

The paper consists of three main parts. Firstly, the description of the system and the model characteristics. Secondly, the analysis of bit stick-slip oscillations and the permanent stuck bit situation. Three key drilling parameters are considered: WOB, the steady rotary speed and the torque applied by the surface motor. In most of drillstrings-control-related works, no bifurcation analysis of the system and the controller parameters is made, and the influence of the WOB is not usually taken into account. The importance of the WOB on the drillstring dynamical behaviour and control was previously established in [17, 18]. Thirdly, two illustrative control methodologies are presented. On the one hand, a linear feedback control is proposed. On the other hand, a discontinuous-type control is used. The controller parameters are chosen so that non-desired system transitions can be avoided.

The bit-sticking scenarios are reinterpreted in terms of a sliding motion present in the system when the bit velocity is zero. The relationships between the sliding motion and the different types of system equilibria will be key elements for studying the open and closed-loop system dynamical behaviours.

2 Torsional behaviour: the most simple discontinuous model

A conventional vertical oilwell drillstring consists of the rotating mechanism at the surface, a set of drill pipes which are screwed one to each other to form a long pipeline, and the BHA. The BHA consists of the drill collars, the stabilizers (at least two spaced apart), a heavy-weighted drill pipe and the bit. While the length of the BHA (L_b) remains constant, the total length of the drill pipeline (L_p) increases as the borehole depth increases and can reach several kilometers (Fig. 1). Hereinafter, the BHA will be also referred to as bit. This paper is focused on the torsional behaviour of this mechanism.

A general lumped-parameter model for the torsional behaviour of drillstrings was proposed in [20]. In the present work, a simplified model of 2 DOF's which appropriately captures the most important dynamical properties is used (Fig. 2). The torsional behaviour model corresponds to a simple torsional pendulum driven by an electrical motor, and the bit-rock contact is described by a dry friction model which includes the WOB. The drill pipes are represented by a linear spring with torsional stiffness k_t and a torsional damping c_t, which

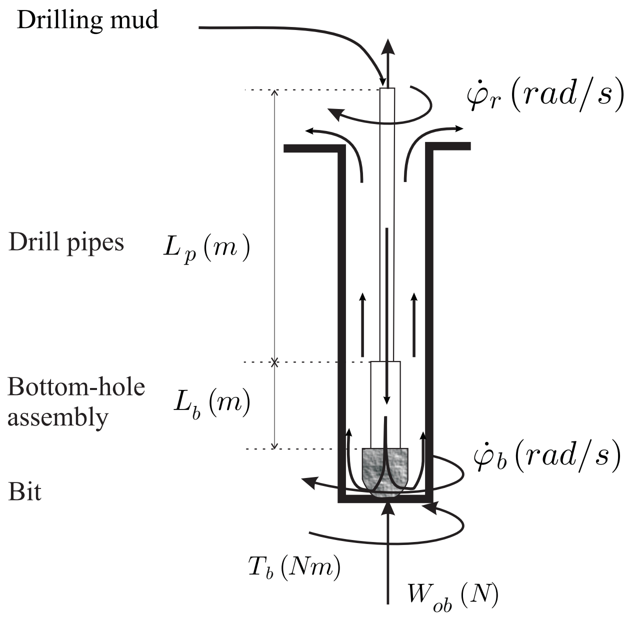

Fig. 1 Important elements in a conventional vertical drillstring (extracted from [20])

connect the inertias J_{r} and J_{b}. J_{b} is usually considered as the sum of the BHA inertia plus one third of the drill pipes [1].

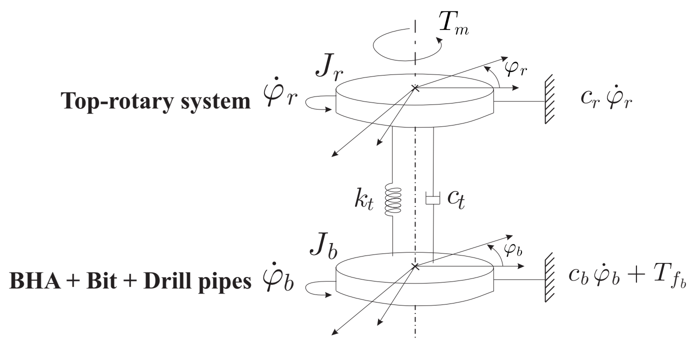

Fig. 2 2-DOF model describing the torsional behaviour of a simplified conventional vertical drillstring

The following assumptions have been made: 1) the borehole and the drillstring are both vertical and straight, 2) no lateral bit motion is present, 3) the friction in the pipe connections and between the pipes and the borehole are neglected, 4) the drilling mud is simplified by a viscous-type friction element at the bit, 5) the drilling mud fluids orbital motion is considered to be laminar, that is, without turbulences, 6) the WOB is constant. Under these assumptions and according to Fig. 2, the equations of motion have the following form:

$$\begin{aligned} J_r\ddot{\varphi}_r + c_t(\dot{\varphi}_r - \dot{\varphi}_b) + k_t(\varphi_r - \varphi_b) &= T_m - T_r(\dot{\varphi}_r) \\ J_b\ddot{\varphi}_b - c_t(\dot{\varphi}_r - \dot{\varphi}_b) - k_t(\varphi_r - \varphi_b) &= -T_b(\dot{\varphi}_b), \end{aligned} \tag{1}$$

with φ_i, $\dot{\varphi}_i$ ($i \in \{r, b\}$) the angular displacements and angular velocities of the drillstring elements, respectively. At the top-drive system, a viscous damping torque is considered ($T_r(\dot{\varphi}_r) = c_r\dot{\varphi}_r$). T_m is the torque applied by the electrical motor at the surface, which is considered constant in this Section and Section 3, with $T_m = u$, where u is the control input.

$T_b(\dot{\varphi}_b) = c_b\dot{\varphi}_b + T_{f_b}(\dot{\varphi}_b)$ is the torque on the bit with $c_b\dot{\varphi}_b$ approximating the influence of the mud drilling on the bit behaviour. $T_{f_b}(\dot{\varphi}_b)$ is the friction modelling the bit-rock contact, and

$$T_{f_b}(\dot{\varphi}_b) = W_{ob}R_b\left[\mu_{c_b} + (\mu_{s_b} - \mu_{c_b})\exp^{-\frac{\gamma_b}{v_f}|\dot{\varphi}_b|}\right]\mathrm{sgn}(\dot{\varphi}_b), \tag{2}$$

with $W_{ob} > 0$ the weight on the bit, $R_b > 0$ the bit radius; μ_{s_b}, $\mu_{c_b} \in (0,1)$ the static and Coulomb friction coefficients associated with J_b, $0 < \gamma_b < 1$ and $v_f > 0$. In addition, the Coulomb and static friction torque is T_{c_b} and T_{s_b}, respectively, with $T_{c_b} = W_{ob}R_b\mu_{c_b}$, $T_{s_b} = W_{ob}R_b\mu_{s_b}$. The form of the friction torque at the bit is appreciated in Fig. 3. The exponential decaying behaviour of the torque on the bit T_b coincides with experimental bit torque values and is inspired in the models given in [1, 12, 13].

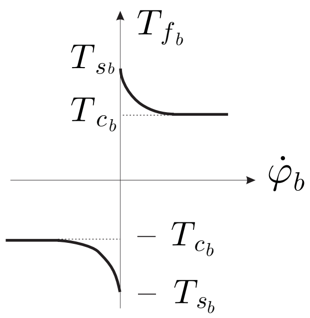

Fig. 3 Friction at the bit (T_{f_b}): dry friction with an exponential-decaying law at the sliding phase. $\dot{\varphi}_b$ (rad/s) bit angular velocity, $T_{s_b} = \mu_{s_b}W_{ob}R_b$ (Nm) static friction torque, $T_{c_b} = \mu_{c_b}W_{ob}R_b$ (Nm) Coulomb friction torque.

In equation (2), the sign function is considered as:

$$\begin{aligned} &\mathrm{sign}(\dot{\varphi}_b) = \dot{\varphi}_b/|\dot{\varphi}_b| && \text{if } \dot{\varphi}_b \neq 0, \\ &\mathrm{sign}(\dot{\varphi}_b) \in [-1,1] && \text{if } \dot{\varphi}_b = 0. \end{aligned} \tag{3}$$

The uncertainty of the system behaviour when the velocity $\dot{\varphi}_b$ is zero is overcome by choosing an adequate mathematical model on the discontinuity surface $\dot{\varphi}_b = 0$. The equivalent dynamics on $\dot{\varphi}_b = 0$ is defined by means of Filippov's continuation method or Utkin's equivalent control method [26, 27].

By defining the system state vector as $\mathbf{x} = (\dot{\varphi}_{\rm r}, \varphi_{\rm r} - \varphi_{\rm b}, \dot{\varphi}_{\rm b})^{\rm T} = (x_1, x_2, x_3)^{\rm T}$, dynamics (1) is rewritten as:

$$\begin{aligned} \dot{x}_1 &= \frac{1}{J_{\rm r}}\left[-(c_{\rm t}+c_{\rm r})x_1 - k_{\rm t}x_2 + c_{\rm t}x_3 + u\right], \\ \dot{x}_2 &= x_1 - x_3, \\ \dot{x}_3 &= \frac{1}{J_{\rm b}}\left[c_{\rm t}x_1 + k_{\rm t}x_2 - (c_{\rm t}+c_{\rm b})x_3 - T_{\rm f_b}(x_3)\right], \end{aligned} \tag{4}$$

or in a compact form: $\dot{\mathbf{x}}(t) = \mathbf{A}\mathbf{x}(t) + \mathbf{B}u + \mathbf{T}_{\rm f}(\mathbf{x}(t))$, where $\mathbf{A}$, $\mathbf{B}$ are constant matrices depending on system parameters and $\mathbf{T}_{\rm f}$ is the vector of the torque on the bit.

In the following simulations, the data corresponding to a real drillstring design reported in [30] are used:

$$\begin{aligned} &J_r = 2122\,kg\,m^2,\, J_b = 471.9698\,kg\,m^2,\, R_b = 0.155575\,m, \\ &k_t = 698.063\,Nm/rad,\, c_t = 139{,}6126\,Nms/rad,\, c_r = 425\,Nms/rad, \\ &c_b = 50\,Nms/rad,\, \mu_{c_b} = 0.5,\, \mu_{s_b} = 0.8,\, D_v = 10^{-6},\, \gamma_b = 0.9,\, v_f = 1. \end{aligned} \tag{5}$$

3 Open-loop system dynamical properties: bit-sticking transitions

Two dynamical properties determine the existence of self-excited bit stick-slip oscillations and permanent stuck bit: 1) the existence of a sliding motion when the bit velocity is zero, 2) the loss of stability of the standard equilibrium of the system, mainly due to the presence of Hopf bifurcations (HB). These phenomena depend on three key drilling parameters: the WOB, the steady rotary speed and the torque applied by the surface motor (u). This section is devoted to analyse these properties, and the conclusions given will be very useful for the selection of the control parameters in Section 4.

System (4) is a piecewise-smooth or switched system which switches from one linear time-invariant configuration to another whenever the bit velocity sign changes, that is,

$$\dot{\mathbf{x}} = \begin{cases} \mathbf{f}^+(\mathbf{x}, W_{\rm ob}, u) = \mathbf{A}\mathbf{x} + \mathbf{B}u + \mathbf{T}_{\rm f}(\mathbf{x})|_{T_{\rm f_b} = T^+_{\rm f_b}} & \text{if } x_3 > 0, \\ \mathbf{f}^-(\mathbf{x}, W_{\rm ob}, u) = \mathbf{A}\mathbf{x} + \mathbf{B}u + \mathbf{T}_{\rm f}(\mathbf{x})|_{T_{\rm f_b} = T^-_{\rm f_b}} & \text{if } x_3 < 0, \end{cases} \tag{6}$$

with,

$$\begin{aligned} T^+_{\rm f_b}(x_3) &= W_{\rm ob}R_{\rm b}\left[\mu_{\rm c_b} + (\mu_{\rm s_b} - \mu_{\rm c_b})\exp^{-\frac{\gamma_{\rm b}}{v_{\rm f}}x_3}\right], \\ T^-_{\rm f_b}(x_3) &= -W_{\rm ob}R_{\rm b}\left[\mu_{\rm c_b} + (\mu_{\rm s_b} - \mu_{\rm c_b})\exp^{\frac{\gamma_{\rm b}}{v_{\rm f}}x_3}\right]. \end{aligned} \tag{7}$$

The switching or discontinuity surface is denoted by $\Sigma_{\rm b}$ and has the form $\Sigma_{\rm b} := \{\mathbf{x} \in \mathbb{R}^3 : \sigma_{\rm b}(\mathbf{x}) = 0\}$, with $\sigma_{\rm b}(\mathbf{x}) = x_3$. On $\Sigma_{\rm b}$, $\mathbf{f}^+(\mathbf{x})$ and $\mathbf{f}^-(\mathbf{x})$ do not agree. The dynamics of the system on $\Sigma_{\rm b}$ is $\dot{\mathbf{x}} = \mathbf{f}_{\rm s}(\mathbf{x})$, and can be obtained by means of the Filippov's continuation method or the Utkin's equivalent control method [26, 27]. Here, the Utkin's equivalent control method is used [27], which, as it is established in [28, 29], gives better chatter-free simulation results for some cases.

It is interesting to notice that T_{f_b} plays the role of the equivalent control (T_{fbeq}), and T_{fbeq} is the solution for T_{f_b} of equation $\dot{x}_3 = 0$, that is, $u_{eq} = T_{fbeq} = c_t x_1 + k_t x_2 - (c_t + c_b) x_3$. Moreover, $-T_{s_b} \leq T_{fbeq} \leq T_{s_b}$. Finally,

$$f_s(\mathbf{x}, u) = \begin{pmatrix} \frac{1}{J_r}\left[-(c_t + c_r)x_1 - k_t x_2 + u\right] \\ x_1 \\ 0 \end{pmatrix}. \tag{8}$$

The quasiequilibrium point existing on Σ_b is denoted by $\tilde{\mathbf{x}}_b$, and is such that $\mathbf{f}_s(\tilde{\mathbf{x}}_b, u) = 0$,

$$\tilde{x}_{b,1} = \tilde{x}_{b,3} = 0, \;\; \tilde{x}_{b,2} = \frac{u}{k_t}. \tag{9}$$

The discontinuity surface Σ_b is divided into two regions, the sliding set $\tilde{\Sigma}_b$, which is closed, and the crossing set Σ_{bc}, which is open. Then $\Sigma_b = \tilde{\Sigma}_b \bigcup \Sigma_{bc}$. $\tilde{\Sigma}_b$ is the set where a sliding motion can take place. On the other hand, Σ_{bc} is the set of Σ_b within which the system trajectory crosses Σ_b without sliding. The crossing set Σ_{bc} is the complement set of $\tilde{\Sigma}_b$ in Σ_b. We have that,

$$\tilde{\Sigma}_b = \{\mathbf{x} \in \Sigma_b : |k_t x_2 + c_t x_1| \leq W_{ob} R_b \mu_{s_b}\}. \tag{10}$$

The boundaries of $\tilde{\Sigma}_b$ are denoted by $\partial\tilde{\Sigma}_b^+$ and $\partial\tilde{\Sigma}_b^-$.

It is assumed that there are no points on $\tilde{\Sigma}_b$ at which both f^+ and f^- are tangent to Σ_b. The sliding set can be attractive or repulsive.

In [20], for an n-DOF drillstring model, $\tilde{\mathbf{x}}_b$ is shown to be asymptotically stable and the relative position of $\tilde{\mathbf{x}}_b$ with respect to the boundary $\partial\tilde{\Sigma}_b^+$ is shown to play a key role in the elimination of bit sticking problems. The bit is ensured to move with a constant positive velocity when $\tilde{\mathbf{x}}_b$ is far away enough from $\partial\tilde{\Sigma}_b^+$, and this is accomplished when u is greater enough than $W_{ob} R_b \mu_{s_b}$.

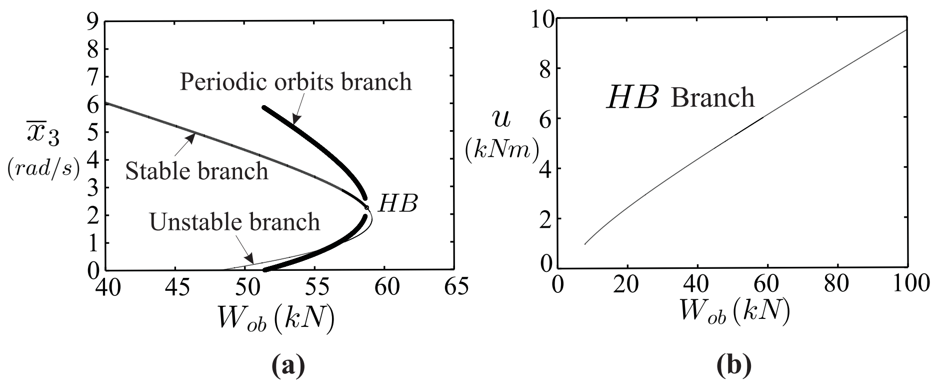

Fig. 4 Bifurcation diagrams for the open-loop system (4): (a) $(W_{ob}, \overline{x}_3)$ for a fixed $u = 6$kNm; (b) values (W_{ob}, u) at which a HB appears. The diagrams have been obtained with XPPAUT [31]

If $x_3 > 0$ then the system has a unique standard equilibrium point $\overline{\mathbf{x}}$ such that $\mathbf{f}^+(\overline{\mathbf{x}}, W_{ob}, u) = 0$, which is the solution of the set of equations:

$$\bar{x}_1 = \bar{x}_3 > 0,\ u - (c_\mathrm{r} + c_\mathrm{b})\bar{x}_3 - T^+_{\mathrm{f_b}}(\bar{x}_3, W_\mathrm{ob}) = 0,\ \bar{x}_2 = \frac{h(\bar{x}_3, W_\mathrm{ob}, u)}{k_\mathrm{t}},$$

with $h(\bar{x}_3, W_\mathrm{ob}, u) = \frac{c_\mathrm{r} T^+_{\mathrm{f_b}}(\bar{x}_3, W_\mathrm{ob}) + c_\mathrm{b} u}{c_\mathrm{r} + c_\mathrm{b}}$ and $u > W_\mathrm{ob} R_\mathrm{b} \mu_{\mathrm{s_b}} > 0$. $\bar{\mathbf{x}}$ loses stability mainly due to the presence of subcritical Hopf bifurcations (HB) for each triple $(W_\mathrm{ob}, u, \bar{x}_3)$.

The stability region of $\bar{\mathbf{x}}$ corresponds to low W_{ob} and high enough values of the steady rotary velocities and the torque u. This can be appreciated in Fig. 4. In Fig. 4.(a), the bifurcation diagram for $(W_\mathrm{ob}, \bar{x}_3)$ for a fixed $u = 6\,\mathrm{kNm}$ is given. The stable branch (the thickest one) represents the values of $(W_\mathrm{ob}, \bar{x}_3)$ for which the system converges to an equilibrium point; whereas the unstable branch represents the values of the parameters for which the system has an unstable equilibrium point. Periodic orbits emanate from HB points. Notice that this bifurcation diagram has been obtained for a fixed u. For each value of u, a different bifurcation diagram can be obtained. This fact is confirmed by Fig. 4.(b) where the values (W_ob, u) at which a HB point is present are depicted. These points are origin of oscillations in the system. For each pair of (W_ob, u) a different periodic orbit can be obtained. The parameters region where stick-slip oscillations are present intersects the parameters region where a HB point may appear.

To conclude with, three main steady behaviours are identified. First, bit stick-slip oscillations (Fig. 5). In this situation, $\bar{\mathbf{x}}$ is unstable or stable with a small domain of attraction, $\tilde{\Sigma}_\mathrm{b}$ alternates between being repulsive and attractive, and $\tilde{\mathbf{x}}_\mathrm{b}$ is close to the boundary of $\tilde{\Sigma}_\mathrm{b}$.

Second, permanent stuck bit, i.e., $\mathbf{x}(t) \in \tilde{\Sigma}_\mathrm{b}, \forall t > \bar{t}$ (Fig. 6). Indeed, the trajectory converges to $\tilde{\mathbf{x}}_\mathrm{b}$. In this case, $\bar{\mathbf{x}}$ is unstable or stable with a small domain of attraction, $\tilde{\Sigma}_\mathrm{b}$ attractive, $\tilde{\mathbf{x}}_\mathrm{b} \in \tilde{\Sigma}_\mathrm{b}$, and $\tilde{\mathbf{x}}_\mathrm{b}$ is far away enough from the boundary $\partial\tilde{\Sigma}^+_\mathrm{b}$ of $\tilde{\Sigma}_\mathrm{b}$.

The third steady behaviour is the trajectory converging to $\bar{\mathbf{x}}$. In this case, $\bar{\mathbf{x}}$ is stable, $\tilde{\Sigma}_\mathrm{b}$ is repulsive, and there are two possibilities:

- $\tilde{\mathbf{x}}_\mathrm{b} \notin \tilde{\Sigma}_\mathrm{b}$ and $\tilde{\mathbf{x}}_\mathrm{b}$ far away enough from the boundary of $\tilde{\Sigma}_\mathrm{b}$, which is accomplished when u is greater enough than $T_{\mathrm{s_b}}$ (Fig. 7.(a)).
- $\tilde{\mathbf{x}}_\mathrm{b} \in \tilde{\Sigma}_\mathrm{b}$ or $\tilde{\mathbf{x}}_\mathrm{b} \notin \tilde{\Sigma}_\mathrm{b}$, and $\tilde{\mathbf{x}}_\mathrm{b}$ is very close to the boundary of $\tilde{\Sigma}_\mathrm{b}$ (Fig. 7.(b)). In this case, the trajectory enters several times the sliding set until it converges to $\bar{\mathbf{x}}$, and consequently, the settling time is higher.

4 The control problem: some solutions

The control goals are to eliminate the bit-sticking phenomena, to drive the bit velocity to a desired value ($\Omega > 0$), and to reduce the influence of key parameters changes. This is achieved by means of different theoretical control methodologies in addition to an adequate selection of controller parameters.

The two control methods proposed in this paper have to be interpreted as off-line safe-parameters selection methods. The model and the controller can help the driller to design, before starting the operation, the well drilling profile with reference values for the torque at the top-rotary system (u), the WOB and desired rotary velocities (Ω). For a combination of (W_{ob}, Ω), the torque u would be obtained so that non-desired bit phenomena can be avoided.

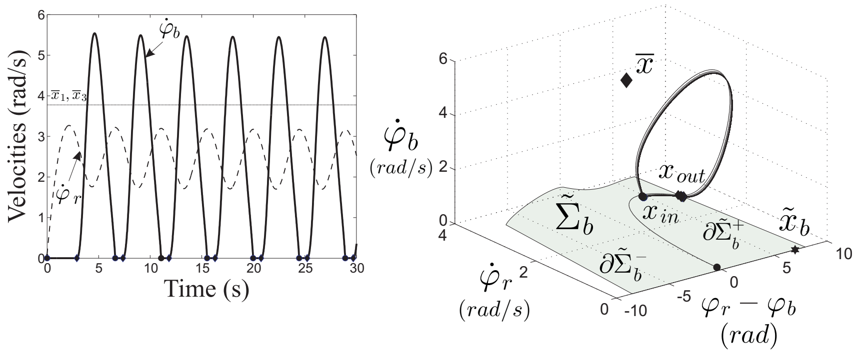

(a) **(b)**

Fig. 5 Stick-slip situation with $W_{\rm ob} = 53018\,N$ and $u = 6\,kNm$: (a) angular displacements and velocities; (b) trajectory of the system in the space $(\varphi_r - \varphi_b, \dot{\varphi}_r, \dot{\varphi}_b)$. $\mathbf{x_{in}}$ (•) and $\mathbf{x_{out}}$ (♦) are the points at which the system trajectory enters and goes out of the sliding set ($\tilde{\Sigma}_{\rm b}$)

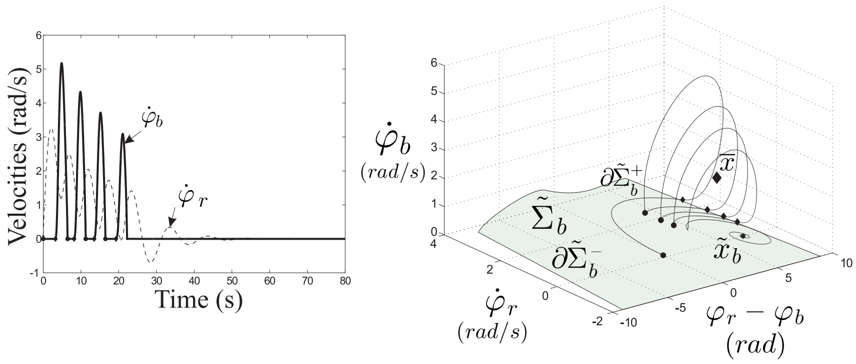

(a) **(b)**

Fig. 6 Permanent stuck bit, the trajectory of the system remains on $\tilde{\Sigma}_{\rm b}$ with $W_{\rm ob} = 59208\,N$, $u = 6\,kNm$: (a) time response; (b) trajectory of the system in the space $(\varphi_r - \varphi_b, \dot{\varphi}_r, \dot{\varphi}_b)$. • $\mathbf{x_{in}}$, ♦ $\mathbf{x_{out}}$

4.1 Proposal of a linear PI-type control

The control goals can be met by using the following proportional-integral (PI) control, with an appropriate selection of controller parameters:

$$
\begin{aligned}
u &= K_1 x_4 + K_2(\Omega - x_1) + K_3(x_1 - x_3) + u^*,\; u^* = T_{s_b},\\
x_4 &= \int_0^t [\Omega - x_1(\tau)]\, d\tau, \qquad (11)\\
\dot{x}_4 &= \Omega - x_1,
\end{aligned}
$$

with $K_{\rm i}$ positive constants and u^* the minimum value of u for the system trajectory to cross the boundary of $\tilde{\Sigma}_{\rm b}$, which prevents the bit from sticking when control (11) is initially switched on.

The closed-loop system is obtained substituting (11) in (4). The closed-loop system state vector is defined as $\mathbf{x}_{\rm c}$, with,

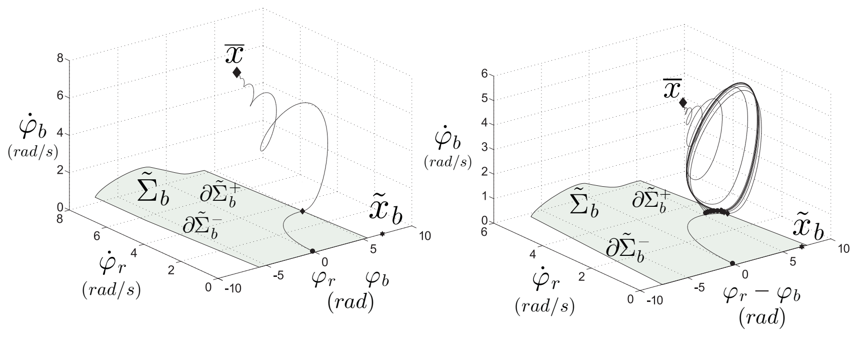

(a) **(b)**

Fig. 7 Different scenarios when $\mathbf{x}(t)$ converges to $\overline{\mathbf{x}}$: (a) $W_{\mathrm{ob}} = 39000N$, $u = 6kNm$, $\tilde{\mathbf{x}}_{\mathrm{b}}$ is outside and far away enough from $\tilde{\Sigma}_{\mathrm{b}}$; (b) $W_{\mathrm{ob}} = 51408N$, $u = 6kNm$, $\tilde{\mathbf{x}}_{\mathrm{b}}$ inside $\tilde{\Sigma}_{\mathrm{b}}$, close to the boundary. • $\mathbf{x_{in}}$, ⧫ $\mathbf{x_{out}}$

$$\mathbf{x}_{\mathrm{c}} = (\dot{\varphi}_{\mathrm{r}}, \varphi_{\mathrm{r}} - \varphi_{\mathrm{b}}, \dot{\varphi}_{\mathrm{b}}, x_4)^{\mathrm{T}} = (x_{\mathrm{c},1}, x_{\mathrm{c},2}, x_{\mathrm{c},3}, x_{\mathrm{c},4})^{\mathrm{T}}.$$

The feedback transformed system has the following form,

$$\dot{\mathbf{x}}_{\mathrm{c}}(t) = \mathbf{A}_{\mathrm{c}}\mathbf{x}_{\mathrm{c}}(t) + \mathbf{T}_{\mathrm{f}}(\mathbf{x}_{\mathrm{c}}(t)), \tag{12}$$

where $\mathbf{A}_{\mathrm{c}}$ is a constant matrix depending on the system parameters.

System (4) with control (11) has a unique standard equilibrium point $\overline{\mathbf{x}}_{\mathrm{c}}$ with velocities equal to Ω, and with $\overline{x}_{\mathrm{c},2}$ and $\overline{x}_{\mathrm{c},4}$ depending on W_{ob} and Ω, that is,

$$\overline{x}_{\mathrm{c},1} = \overline{x}_{\mathrm{c},3} = \Omega, \tag{13}$$

$$\overline{x}_{\mathrm{c},2} = \frac{h(\Omega)}{k_{\mathrm{t}}},\ h(\Omega) = \left[c_{\mathrm{b}}\Omega + T^{+}_{\mathrm{f_b}}(\Omega)\right], \tag{14}$$

$$\overline{x}_{\mathrm{c},4} = \frac{1}{K_1}\left[(c_{\mathrm{r}} + c_{\mathrm{b}})\Omega + T^{+}_{\mathrm{f_b}}(\Omega) - u^{*}\right] \tag{15}$$

with $T^{+}_{\mathrm{f_b}}$ as defined in (7).

In the controlled system, the conditions for the existence of the sliding motion on Σ_{b} are not modified by control (11). The sliding set (10) is maintained. The dynamics of the closed-loop system on Σ_{b} is obtained by means of the Utkin's equivalent control method [27] and has the form,

$$\mathbf{f}_{\mathrm{sc}}(\mathbf{x}_{\mathrm{c}}, W_{\mathrm{ob}}, K_{\mathrm{i}}) = \mathbf{A}_{\mathrm{c}}\mathbf{x}_{\mathrm{c}} + \mathbf{T_f}(\mathbf{x}_{\mathrm{c}})|_{T_{f_b} = T_{fbeq}}, \tag{16}$$

where

$$T_{fbeq}(\mathbf{x}_{\mathrm{c}}) = c_{\mathrm{t}}x_{\mathrm{c},1} + k_{\mathrm{t}}x_{\mathrm{c},2} - (c_{\mathrm{t}} + c_{\mathrm{b}})x_{\mathrm{c},3}. \tag{17}$$

Now, there is no $\tilde{\mathbf{x}}_{\mathrm{c}}$ such that $\mathbf{f}_{\mathrm{sc}}(\tilde{\mathbf{x}}_{\mathrm{c}}, W_{\mathrm{ob}}, K_{\mathrm{i}}) = 0$. Therefore, there is no quasiequilibrium point in the closed-loop system, and the permanent stuck-bit situation is avoided, whereas stick-slip oscillations may appear.

To conclude with, there are four main dynamical features in the closed-loop system. First, the standard equilibrium point has the angular velocities equal to the positive desired velocity

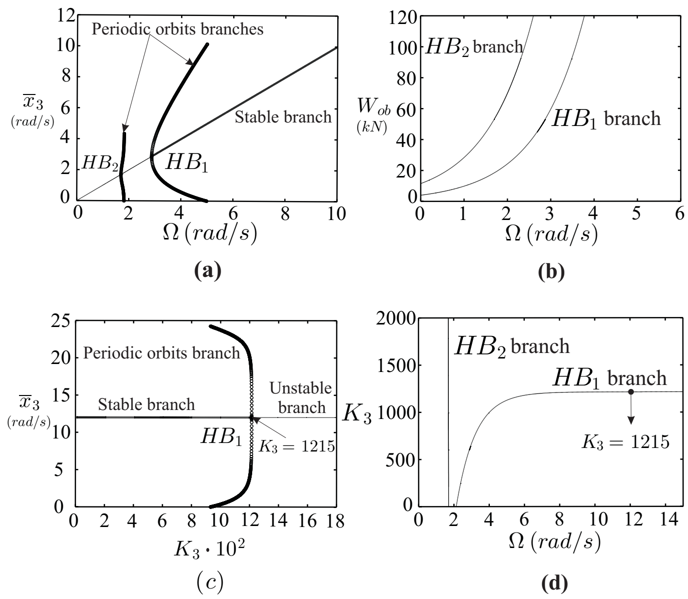

Fig. 8 Bifurcation diagrams for the closed-loop system with the PI-type controller: (a) fixed $W_{ob} = 53018\,\mathrm{N}$, $K_3 = 600$; (b) fixed $K_3 = 600$; (c), (d) fixed $W_{ob} = 53018\,\mathrm{N}$. The diagrams have been obtained with XPPAUT [31]

Ω. Second, the sliding motion on Σ_b is maintained. Third, there is no quasiequilibrium point on Σ_b, thus, the permanent stuck-bit situation is eliminated. Finally, stick-slip oscillations may still arise due to the loss of stability of $\overline{\mathbf{x}}_c$. The equilibrium loses stability mainly to the presence of two Hopf bifurcations which give rise to branches of unstable periodic orbits for low Ω, high W_{ob} and high K_3 (close to the value $K_3 = 1215$). These facts can be appreciated from Fig. 8 in which fixed $K_1 = 15$, $K_2 = 10$ are used. The paper [23] gives more details on the stability analysis of the closed-loop system, as well as guidelines to select the controller parameters K_i.

According to Figs. 8.(a) and 8.(d), the fact of having the velocity Ω close to the interval $[2\,\mathrm{rad/s}, 5\,\mathrm{rad/s}]$ leads to the unstability of $\overline{\mathbf{x}}_c$ and the presence of stick-slip oscillations, as Figs. 9.(a) and 9.(b) show.

4.2 Discontinuous control: sliding-mode control

The control strategy consists in inserting an attractive surface of discontinuity, $\sigma_r = 0$, along which the system exhibits the desired dynamics. For this purpose, a discontinuous control is proposed so that the system trajectory reaches this surface and enters a sliding motion. Thus, the following functions are proposed [22, 32]:

$$\begin{aligned}\sigma_r(\mathbf{x},t) &= (x_1-\Omega)+\lambda\int_0^t [x_1(\tau)-\Omega]\,d\tau+\lambda\int_0^t [x_1(\tau)-x_3(\tau)]\,d\tau,\ \lambda>0,\\ u &= c_t(x_1-x_3)+k_t x_2+c_r x_1-J_r\left[\lambda(x_1-\Omega)+\lambda(x_1-x_3)+\eta\, sign(\sigma_r)\right],\ \eta>0,\end{aligned} \tag{18}$$

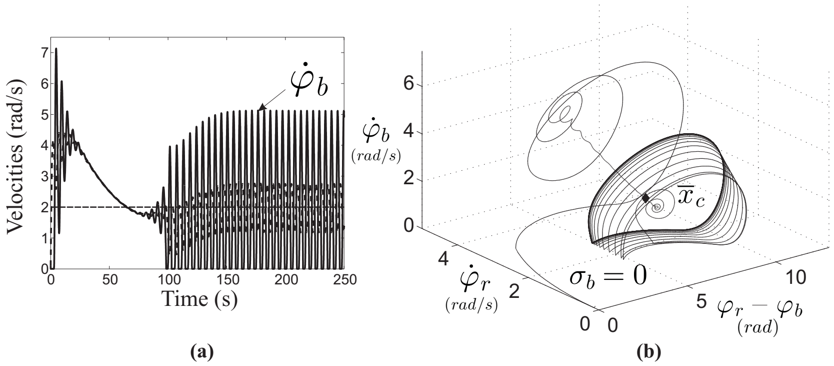

Fig. 9 Stick-slip oscillations appear when $\Omega = 2\,\mathrm{rad/s}$, $W_{\mathrm{ob}} = 53018\,\mathrm{N}$: response for the PI-type control (11) with $u^* = T_{\mathrm{s_b}}$, $K_1 = 15$, $K_2 = 10$, $K_3 = 20$. $\bar{\mathbf{x}}_{\mathrm{c}}$ is unstable

where, again, $\Omega > 0$ is the desired rotary velocity. Furthermore, $\sigma_{\mathrm{r}}(\mathbf{x},t)$ becomes zero in a finite time interval $t_{\mathrm{sr}} = \frac{|\sigma_{\mathrm{r}}(\mathbf{x},t_0)|}{\eta}$. Two new states x_4, x_5 are defined, such that, $\dot{x}_4 = x_1 - \Omega$ and $\dot{x}_5 = x_1 - x_3$. Control (18) was previously proposed in [22] for a 4-DOF drillstring and in [32] was rewritten for the 2-DOF model considered in this paper.

The following switching surface is defined: $\Sigma_{\mathrm{r}} := \{\mathbf{x} \in \mathbb{R}^5 : \ \sigma_{\mathrm{r}}(\mathbf{x},t) = 0\}$. This surface has been designed in such a way to be attractive for all $\mathbf{x}$ and to be a sliding set for all $\mathbf{x} \in \Sigma_{\mathrm{r}}$. According to (18), control u is of swiched type, with the form:

$$u = \begin{cases} u^+ \text{ if } \sigma_{\mathrm{r}} > 0 \\ u^- \text{ if } \sigma_{\mathrm{r}} < 0 \end{cases}, \tag{19}$$

and u^+ and u^- are obtained by changing the sign of σ_{r} in (18). The equivalent control that makes the trajectories evolve on Σ_{r} is $u^- < u^{\mathrm{r}}_{\mathrm{eq}} < u^+$, with:

$$u^{\mathrm{r}}_{\mathrm{eq}}(\mathbf{x}) = c_{\mathrm{t}}(x_1 - x_3) + k_{\mathrm{t}}x_2 + c_{\mathrm{r}}x_1 - J_{\mathrm{r}}\left[\lambda(x_1 - \Omega) + \lambda(x_1 - x_3)\right]. \tag{20}$$

Consequently, the dynamics on Σ_{r} has the following form:

$$\dot{\mathbf{x}} = f^{\mathrm{r}}_{\mathrm{s}}(\mathbf{x},u)|_{u=u^{\mathrm{r}}_{\mathrm{eq}}} = \begin{pmatrix} -\lambda(x_1 - \Omega) - \lambda(x_1 - x_3) \\ x_1 - x_3 \\ \frac{1}{J_{\mathrm{b}}}\left[c_{\mathrm{t}}x_1 + k_{\mathrm{t}}x_2 - (c_{\mathrm{t}} + c_{\mathrm{b}})x_3 - T_{\mathrm{f_b}}(x_3)\right] \\ x_1 - \Omega \\ x_1 - x_3 \end{pmatrix}.$$

In addition, control u has modified the dynamics on Σ_{b}, and now, the equivalent dynamics on Σ_{b} is:

$$\dot{\mathbf{x}} = f^{\mathrm{b}}_{\mathrm{s}}(\mathbf{x}) = \begin{pmatrix} -2\lambda x_1 + \lambda\Omega - \eta\,\mathrm{sign}(\sigma_{\mathrm{r}}) \\ x_1 \\ 0 \\ x_1 - \Omega \\ x_1 \end{pmatrix}.$$

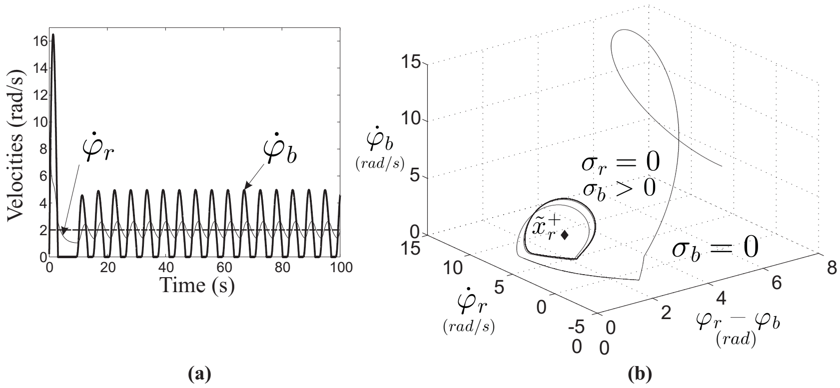

Fig. 10 Stick-slip oscillations appear when $\Omega = 2\,\text{rad/s}$, $W_{\text{ob}} = 53018\,\text{N}$: response for the sliding-mode-based control (18) with $\lambda = 0.3$, $\eta = 3$. $\tilde{\mathbf{x}}_{\text{r}}^{+}$ is unstable

We are going to assume that the velocity x_3 is always positive, so, the situations of having $\sigma_{\text{b}} < 0$ are not considered.

To conclude with, there are three main dynamical changes introduced by control (18) in the open-loop system (4). First, the elimination of the standard equilibrium point $\bar{\mathbf{x}}$. Second, there is only one equilibrium in the system, the quasiequilibrium point $\tilde{\mathbf{x}}_{\text{r}}^{+}$ with velocities equal to Ω, which can become unstable for $\Omega < \Omega^*$, with Ω^* some positive velocity. For more details on the study of the stability of $\tilde{\mathbf{x}}_{\text{r}}^{+}$, the reader is invited to read [22].

Finally, the closed-loop system has multiple switching surfaces, which have the form:

$$
\begin{aligned}
\Sigma_{\text{r}}^{+} &:= \{\mathbf{x} \in \mathbb{R}^5, t \geq t_{\text{sr}} :\ \sigma_{\text{r}}(\mathbf{x},t) = 0, \sigma_{\text{b}}(\mathbf{x}) > 0\},\\
\Sigma_{\text{rb}} &:= \{\mathbf{x} \in \mathbb{R}^5, t \geq t_{\text{sr}} :\ \sigma_{\text{r}}(\mathbf{x},t) = 0, \sigma_{\text{b}}(\mathbf{x}) = 0\},\\
\Sigma_{\text{b}}^{+} &:= \{\mathbf{x} \in \mathbb{R}^5, t < t_{\text{sr}} :\ \sigma_{\text{r}}(\mathbf{x},t) > 0, \sigma_{\text{b}}(\mathbf{x}) = 0\},\\
\Sigma_{\text{b}}^{-} &:= \{\mathbf{x} \in \mathbb{R}^5, t < t_{\text{sr}} :\ \sigma_{\text{r}}(\mathbf{x},t) < 0, \sigma_{\text{b}}(\mathbf{x}) = 0\}.
\end{aligned}
$$

The vector fields associated to the dynamics of the system along these surfaces are:

$$
\mathbf{f}_{\Sigma_{\text{r}}^{+}}(\mathbf{x}, W_{\text{ob}}, \Omega, \lambda) = \begin{pmatrix} -\lambda(x_1 - \Omega) - \lambda(x_1 - x_3) \\ x_1 - x_3 \\ \frac{1}{J_{\text{b}}}\left[\varphi(\mathbf{x}) - T_{\text{f}_{\text{b}}}^{+}(x_3)\right] \\ x_1 - \Omega \\ x_1 - x_3 \end{pmatrix}, \mathbf{f}_{\Sigma_{\text{rb}}}(x_1, \Omega, \lambda) = \begin{pmatrix} -2\lambda x_1 + \lambda\Omega \\ x_1 \\ 0 \\ x_1 - \Omega \\ x_1 \end{pmatrix},
$$

$$
\mathbf{f}_{\Sigma_{\text{b}}^{+}}(x_1, \Omega, \lambda, \eta) = \begin{pmatrix} -2\lambda x_1 + \lambda\Omega - \eta \\ x_1 \\ 0 \\ x_1 - \Omega \\ x_1 \end{pmatrix}, \mathbf{f}_{\Sigma_{\text{b}}^{-}}(x_1, \Omega, \lambda, \eta) = \begin{pmatrix} -2\lambda x_1 + \lambda\Omega + \eta \\ x_1 \\ 0 \\ x_1 - \Omega \\ x_1 \end{pmatrix},
$$

with $\varphi(\mathbf{x}) = c_{\text{t}} x_1 + k_{\text{t}} x_2 - (c_{\text{t}} + c_{\text{b}}) x_3$.

It is obtained that $\tilde{\mathbf{x}}_{\text{r}}^{+} \in \Sigma_{\text{r}}^{+}$. There are two possible dynamical scenarios depending on the stability of $\tilde{\mathbf{x}}_{\text{r}}^{+}$:

- $\tilde{\mathbf{x}}_r^+$ is unstable for $\Omega < \Omega^*$, then the trajectory alternates sliding on Σ_{rb} and Σ_r^+. In this case, stick-slip oscillations appear (Fig. 10).
- $\tilde{\mathbf{x}}_r^+$ is asymptotically stable for $\Omega \geq \Omega^*$, then the trajectory stays on Σ_r^+ converging to $\tilde{\mathbf{x}}_r^+$. This is the desired situation (Fig. 11).

The local asymptotic stability of $\tilde{\mathbf{x}}_r^+$ can be ensured by means of the Routh-Hurwitz criterion and an estimation of Ω^* can be obtained. For parameters (5), and typical values of W_{ob}, Ω^* is close to $4\,\mathrm{rad/s}$. Taking into account that typical operation rotary velocities are $8\,\mathrm{rad/s} < \Omega < 14\,\mathrm{rad/s}$, the controller proposed is valid [22].

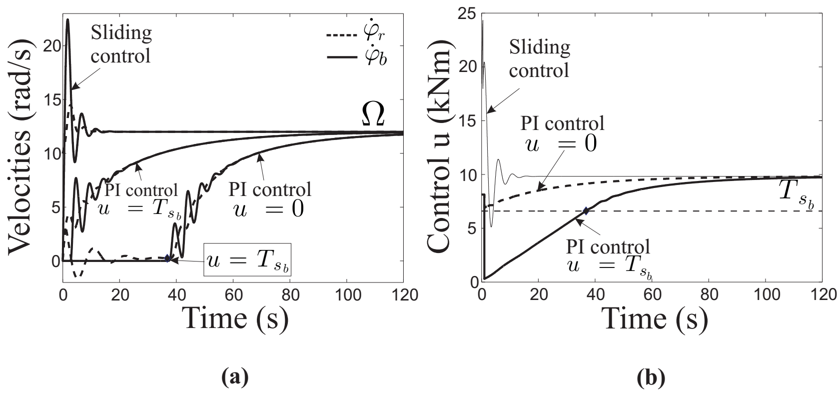

Fig. 11 The control goal is achieved for $\Omega = 12\,\mathrm{rad/s}$: (a) velocities for the three controls; (b) control. The same parameters as those in Fig. 10 are used. $\tilde{\mathbf{x}}_r^+$ is asymptotically stable

Similar results are obtained with the two control strategies (compare Figs. 9, 10 and 11). The main conclusion is that for high enough velocities Ω and low enough W_{ob}, the system trajectories converge to an equilibrium with the velocities equal to the desired value $\Omega > 0$, despite the presence of sliding motions.

5 Closing remarks

The analysis and control of complex behaviour in a class of discontinuous electromechanical systems with dry friction has been carried out. In particular, the analysis and control of bit sticking phenomena in a simplified model of a conventional vertical oilwell drillstring. The analysis of bit dynamical transitions has been used to propose operation recommendations and drilling parameters selection methods in order to reduce non-desired oscillations and bit phenomena. A non-classical nonlinear control technique, such as, sliding-mode-based control has been applied together with a classical proportional-integral linear scheme. In order to select the controller parameters, a bifurcation analysis has been carried out. The analysis can be successfully applied to multi-degree-of-freedom mechanical systems exhibiting stick-slip oscillations and dry friction.

References

1. J.F. Brett. The genesis of torsional drillstring vibrations. *SPE Drilling Engineering*, September:168–174, 1992.
2. S.L. Chen, K. Blackwood and E. Lamine. Field investigation of the effects of stick-slip, lateral and whirl vibrations on roller-cone bit performance. *SPE Drilling and Completion*, 17(1):15–20, 2002.
3. A.P. Christoforou and A.S. Yigit. Fully coupled vibrations of actively controlled drillstrings. *Journal of Sound and Vibration*, 267:1029–1045, 2003.
4. E.M. Navarro-López and R. Suárez-Cortez. Vibraciones mecánicas en una sarta de perforación: Problemas de control. *Revista Iberoamericana de Automática e Informática Industrial*, 2(1):43–54, 2005.
5. H. Henneuse. Surface detection of vibrations and drilling optimization: Field experience. In *Proceedings of the IADC/SPE Drilling Conference*, pages 409–423, 1998.
6. P.C. Kriesels, W.J.G. Keultjes, P. Dumont, I. Huneidi, A. Furat, O.O. Owoeye and R.A. Hartman. Cost savings through an integrated approach to drillstrin vibration control. In *Proceedings of the Middle East Drilling Technology Conference*, SPE/IADC 57555, 1999.
7. Y.-Q. Lin and Y.-H. Wang. Stick-slip vibration of drill strings. *Journal of Engineering Industry*, 113:38–43, 1991.
8. J.D. Macpherson, P.N Jogi and J.E.E. Kingman. Application and analysis of simultaneous near bit and surface dynamics measurements. *SPE Drilling and Completion*, 16(4):230–238, 2001.
9. J.D. Jansen and L. van den Steen. Active damping of self-excited torsional vibrations in oil well drillstrings. *Journal of Sound and Vibration*, 179(4):647–668, 1995.
10. G.W. Halsey, Å. Kyllingstad and A. Kylling. Torque feedback used to cure slip-stick motion. In *Proceedings of the 63rd SPE Annual Technical Conference and Exhibition*, pages 277–282, 1988.
11. P. Sananikone, O. Kamoshima and D.B. White. A field method for controlling drillstring torsional vibrations. In *Proceedings of the IADC/SPE Drilling Conference*, New Orleans, USA, pages 443–452, 1992.
12. F. Abbassian and V.A. Dunayevsky. Application of stability approach to torsional and lateral bit dynamics. *SPE Drilling and Completion*, 13(2):99–107, 1998.
13. D.R. Pavone and J.P. Desplans. Application of high sampling rate downhole measurements for analysis and cure of stick-slip in drilling. In *SPE Annual Technical Conference and Exhibition*, New Orleans, USA, pages 335–345, 1994.
14. A.S. Yigit and A.P. Christoforou. Coupled torsional and bending vibrations of actively controlled drillstrings. *Journal of Sound and Vibration*, 234(1):67–83, 2000.
15. A.F.A. Serrarens, M.J.G. van de Molengraft, J.J. Kok and L. van den Steen. H_∞ control for suppressing stick-slip in oil well drillstrings. *IEEE Control Systems Magazine*, April:19–30, 1998.
16. E.M. Navarro-López. *Notas acerca del modelado, análisis y control de las vibraciones mecánicas en una sarta de perforación*. Drilling monograph, Mexican Institute of Petroleum, June, 2003.
17. E.M. Navarro-López and R. Suárez. Vibraciones en una sarta de perforación: Problemas de control. In *Proceedings of the 11th Latin American Congress of Automatic Control*, La Habana, Cuba, May, 2004.
18. E.M. Navarro-López and R. Suárez-Cortez. Practical approach to modelling and controlling stick-slip oscillations in oilwell drillstrings. In *Proceedings IEEE International Conference on Control Applications*, Taipei, Taiwan, September 2–5, pages 1454–1460, 2004.
19. E.M. Navarro-López and R. Suárez. Modelling and analysis of stick-slip behaviour in a drillstring under dry friction. In *Proceedings of the Congress of the Mexican Association of Automatic Control*, Mexico, D.F., October, pages 330–335, 2004.
20. E.M Navarro-López and D. Cortés. Avoiding harmful oscillations in a drillstring through dynamical analysis. *Journal of Sound and Vibration*, 307(1-2):152–171, 2007.
21. E.M Navarro-López and D. Cortés. Controller parameters selection through bifurcation analysis in a piecewise-smooth system. In *Proceedings HSCC 2007, LNCS 4416*, pages 736–740, Springer-Verlag, Berlin, 2007.

22. E.M. Navarro-López and E. Licéaga-Castro. Non-desired transitions and sliding-mode control of a multi-DOF mechanical system with stick-slip oscillations. *Chaos, Solitons & Fractals*, 41:2035–2044, 2009.
23. E.M. Navarro-López. An alternative characterization of bit-sticking phenomena in a multi-degree-of-freedom controlled drillstring. *Nonlinear Analysis: Real World Applications*, 79:796–802, 2009.
24. E.M. Navarro-López. Hybrid modelling of a discontinuous dynamical system including switching control. In *Proceedings 2nd IFAC Conference on Analysis and Control of Chaotic Systems*, special session *Dynamics of piecewise smooth systems*, London, United Kingdom, June 22–24, 2009.
25. E.M. Navarro-López. Hybrid-automaton models for simulating systems with sliding motion: still a challenge. *3rd IFAC Conference on Analysis and Design of Hybrid Systems*, Zaragoza, Spain, September 16–18, 2009.
26. A.F. Filippov. *Differential equations with discontinuous right-hand sides*. Kluwer Academic Publishers, Dordrecht, 1988.
27. V.I. Utkin. *Sliding modes in control optimization*. Springer-Verlag, Berlin, 1992.
28. P.J. Mosterman, F. Zhao and G. Biswas. Sliding mode model semantics and simulation for hybrid systems. *P. Antsaklis et al. (Eds); Hybrid Systems V, LNCS*, 1567:218–237, Springer-Verlag, 1999.
29. F. Zhao and V.I. Utkin. Adaptive simulation and control variable-structure control systems in sliding regimes. *Automatica*, 32(7):1037–1042, 1996.
30. Tri-cone manual de barrenas. USA: Hughes Tool Company, 1982.
31. B. Ermentrout. *Simulating, analyzing, and animating dynamical systems (A guide to XPPAUT for researchers and students)*. SIAM Software Environments Tools, 2002.
32. E.M. Navarro-López. Discontinuities-induced phenomena in an industrial application: analysis and control solutions. In *Proceedings of the ICNPAA 2008, 7th International Conference on Mathematical Problems in Engineering, Aerospace and Sciences*, Genoa, Italy, June 24–27, 2008.